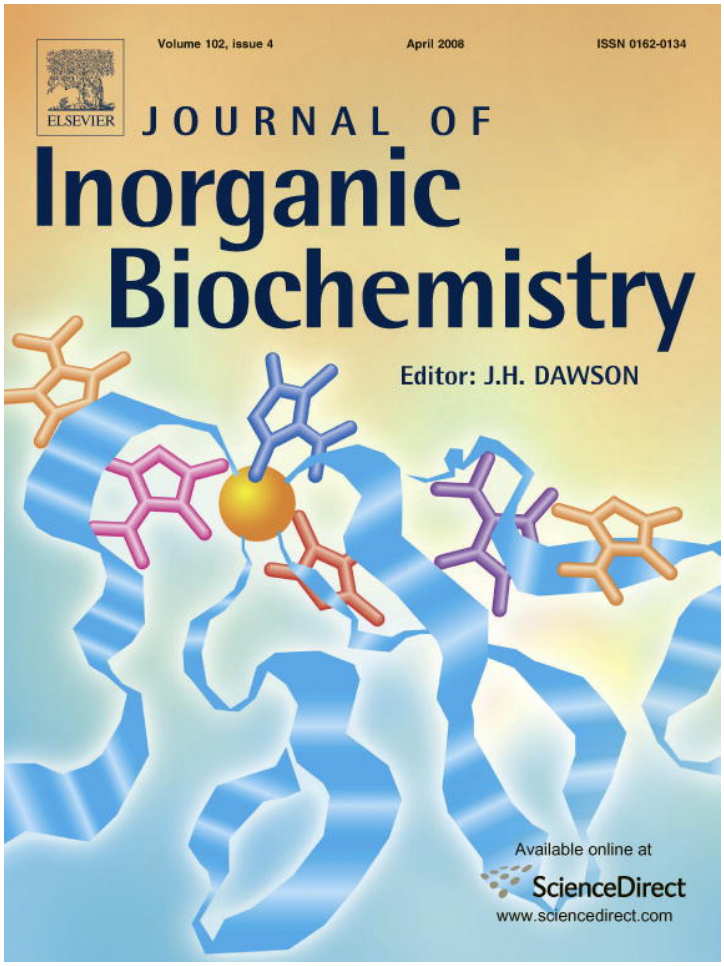

Available online at www.sciencedirect.com
ScienceDirect
Journal of Inorganic Biochemistry 102 (2008) 824–832
Journal of Inorganic Biochemistry
www.elsevier.com/locate/jinorgbio

Oxidative DNA cleavage by Schiff base tetraazamacrocyclic oxamido nickel(II) complexes

De-Ming Kong [a,c,*], Jiao Wang [a], Li-Na Zhu [b,1], Ya-Wei Jin [c], Xiao-Zeng Li [b], Han-Xi Shen [c], Huai-Feng Mi [a]

[a] Key Laboratory of Functional Polymer Materials (Nankai University), Ministry of Education, Nankai University, Tianjin 300071, PR China
[b] Department of Chemistry, Tianjin University, Tianjin 300072, PR China
[c] Research Centre for Analytical Sciences, Department of Chemistry, Nankai University, Tianjin 300071, PR China

Received 29 August 2007; received in revised form 23 October 2007; accepted 7 December 2007
Available online 23 December 2007

Abstract

Nickel is considered a weak carcinogen. Some researches have shown that bound proteins or synthetic ligands may increase the toxic effect of nickel ions. A systematic study of ligand effects on the interaction between nickel complexes and DNA is necessary. Here, we compared the interactions between DNA and six closely related Schiff base tetraazamacrocyclic oxamido nickel(II) complexes $NiL^{1-3a,1-3b}$. The structure of one of the six complexes, NiL^{3b} has been characterized by single crystal X-ray analysis. All of the complexes can cleave plasmid DNA under physiological conditions in the presence of H_2O_2. NiL^{3b} shows the highest DNA cleavage activity. It can convert supercoiled DNA to nicked DNA then linear DNA in a sequential manner as the complex concentration or reaction time is increased. The cleavage reaction is a typical pseudo-first-order consecutive reaction with the rate constants of $3.27 \pm 0.14\ h^{-1}$ (k_1) and $0.0966 \pm 0.0042\ h^{-1}$ (k_2), respectively, when a complex concentration of 0.6 mM is used. The cleavage mechanism between the complex and plasmid DNA is likely to involve hydroxyl radicals as reactive oxygen species. Circular dichronism (CD), fluorescence spectroscopy and gel electrophoresis indicate that the complexes bind to DNA by partial intercalative and groove binding modes, but these binding interactions are not the dominant factor in determining the DNA cleavage abilities of the complexes.

Keywords: Schiff base tetraazamacrocyclic oxamido nickel(II) complexes; Plasmid DNA; Oxidative DNA cleavage; Ligands effect; Binding mode

1. Introduction

Identifying small molecules that are capable of binding and cleaving DNA has attracted considerable interest over the last few decades [1]. Such inexpensive small-molecule catalysts would potentially be valuable tools in biotechnology, nanotechnology, therapeutic approaches and the study of nucleic acid conformations. In this regard, metal complexes have been found to be particularly useful because of their potential to bind DNA via a multitude of interactions and to cleave the duplex [2]. The hydrolytic and oxidative cleavage of supercoiled plasmid DNA by various metal complexes has been widely reported [3].

Nickel complexes draw much attention due to the environmental toxicity and carcinogenic nature of certain nickel compounds and the chemotherapentic properties of other group VIII metal complexes [4]. Some researches have shown that bound proteins or synthetic ligands may increase the toxic effect of nickel ions. However, up to now, the exact mechanism to involve carcinogenesis has not been fully elucidated [5]. The elucidation of the mechanism is essential not only for the risk assessment [6], but

* Corresponding author. Address: Key Laboratory of Functional Polymer Materials (Nankai University), Ministry of Education, Nankai University, Tianjin 300071, PR China. Tel.: +86 22 23505244; fax: +86 22 23502458.
E-mail addresses: kongdem@nankai.edu.cn (D.-M. Kong), linazhu@tju.edu.cn (L.-N. Zhu).
[1] Fax: +86 22 27403475.

0162-0134/$ - see front matter © 2007 Elsevier Inc. All rights reserved.
doi:10.1016/j.jinorgbio.2007.12.002

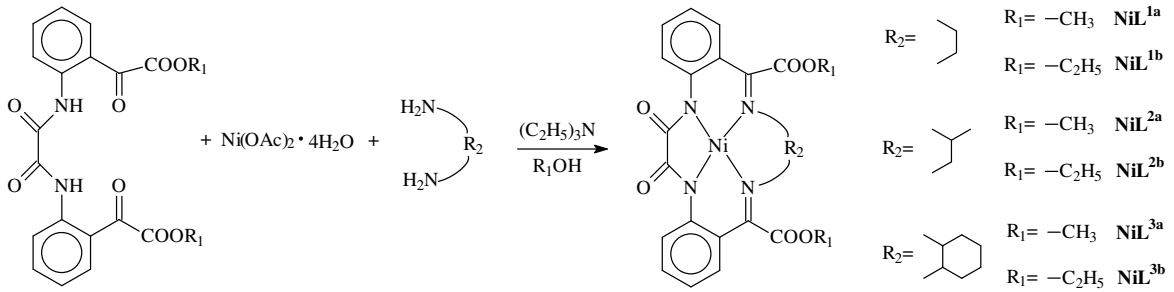

Scheme 1. The synthetic route and schematic structures of the Schiff base tetraazamacrocyclic oxamido nickel(II) complexes.

also for developing novel nickel complexes that have potential applications in medicine and research, such as inhibitors of cancer proliferation and useful DNA or RNA probes [7,8]. Therefore, further studies by employing various ligands with different structures to evaluate and understand those factors that can determine the DNA-binding modes and cleavage mechanism are necessary.

Schiff base complexes present suitable biometric properties that can mimic the structural features of the active sites, and they have been wildly used in various fields such as illness treatment, biochemical reaction and biological regulator [9]. Muller et al. systematically investigated ligand effects, such as ring size, redox potential, ligand donor strength and conformational flexibility, of tetraazamacrocyclic nickel(II) complexes on their DNA cleavage abilities [4]. Such studies may define the important criteria for design of nickel-based reagents as structural probes of nucleic acid. It has been widely reported that the interaction between metal complexes and DNA, such as electrostatic interaction, intercalative binding, and groove binding, may have great effects on the DNA cleavage activities of the metal complexes [10,11]. Systematic investigation of these factors on the DNA cleavage activities of tetraazamacrocyclic Schiff base nickel(II) complexes may supplement important information for design of nickel-base DNA probes. In this paper, we synthesized six closely related Schiff base tetraazamacrocyclic oxamido nickel(II) complexes $NiL^{1-3a,\,1-3b}$ (Scheme 1), where NiL^{3a} is a new compound and the structure of NiL^{3b} is firstly characterized by single crystal X-ray analysis. The cleavage behavior toward pBR 322 DNA of these nickel(II) complexes were compared, and their binding properties to calf thymus DNA (CT DNA) were studied using CD spectroscopy and fluorescence spectroscopy.

2. Materials and methods

2.1. Materials

All material and solvents were purchased commercially and used without further purification unless otherwise noted. CT DNA was dissolved in distilled water and the concentration was determined by absorption spectroscopy using the molar absorption coefficient (6600 $M^{-1}\,cm^{-1}$) at 260 nm. The solution gave a ratio of ultraviolet (UV) absorbance at 260 and 280 nm of ~1.83:1, indicating that the DNA was sufficiently free of protein.

2.2. Synthesis of the Schiff base macrocyclic oxamido nickel(II) complexes

The precursor ligands dimethyl 2,2′-(oxalyldiimino)bis(phenylglyoxylate), diethyl 2,2′-(oxalyldiimino)bis-(phenylglyoxylate), and all complexes were prepared by the literature method [12]. The synthetic route was shown in Scheme 1. The detailed synthetic procedure of NiL^{3a} and NiL^{3b} was as follows.

2.2.1. NiL^{3a}

The mixture of dimethyl 2,2′-(oxalyldiimino)bis(phenylglyoxylate) (2.0 mmol), ±-1,2-cyclohexanediamine (70%, 2.0 mmol), $Ni(Ac)_2 \cdot 4H_2O$ (2.0 mmol), methanol (30 mL) and triethylamine (1.2 mL) was refluxed for 5 h under continuous stirring. The resulted solid was recrystallized in methanol and the red microcrystal of NiL^{3a} was obtained. Yield: 28%. Analysis calculated for $C_{26}H_{24}N_4NiO_6$ (M = 547.19): C 57.07, H 4.42, N 10.24; Found: C 57.31, H 4.55, N 10.16%. Main IR bands: 1740 cm^{-1} (C=O, ester), 1671 cm^{-1} (C=O, oxamido), 1610 and 1590 cm^{-1} (C=N).

2.2.2. NiL^{3b}

Using diethyl 2,2′-(oxalyldiimino)bis (phenylglyoxylate) and ethanol, NiL^{3b} was obtained. The red block single crystal suitable for X-ray analysis was obtained by slow evaporation of the ethanol solution of NiL^{3b} at room temperature. Yield: 23%. Analysis calculated for $C_{28}H_{28}N_4NiO_6$ (M = 575.25): C 58.46, H 4.91, N 9.74; Found: C 58.32, H 4.86, N 9.93%. Main IR bands: 1734 cm^{-1} (C=O, ester), 1676 cm^{-1} (C=O, oxamido), 1608 and 1591 cm^{-1} (C=N).

2.3. X-ray crystallographic study of NiL^{3b}

Diffraction measurements for the single crystal of NiL^{3b} were made on a Rigaku Saturn CCD area detector with graphite monochromated Mo Kα radiation by ω scans technique. Data were collected and processed using CrystalClear (Rigaku). The structure was solved using the direct

Table 1
Crystal data and structure refinement summary for NiL[3b]

Empirical formula	$C_{28}H_{28}N_4NiO_6$
Formula weight	575.25
Temperature	113(2) K
Wavelength	0.71070 Å
Crystal system	Monoclinic
Space group	$P2_1/n$
Unit cell dimensions	$a = 15.391(3)$ Å, $\alpha = 90°$ $b = 9.5408(15)$ Å, $\beta = 105.961(2)°$ $c = 17.923(3)$ Å, $\gamma = 90°$
Volume	2530.4(7) Å^3
Z, Calculated density	4, 1.510 g cm^{-3}
Absorption coefficient	0.819 mm^{-1}
$F(000)$	1200
Crystal size	0.14 × 0.12 × 0.08 mm
θ range for data collection	2.05°–27.87°
Index ranges	$-20 \le h \le 14$, $-12 \le k \le 12$, $-23 \le l \le 23$
Reflection collected/unique	23,332/6032 [$R_{int} = 0.0463$]
Completeness to $\theta = 27.87°$	99.9%
Absorption correction	Semi-empirical from equivalents
Refinement method	Full-matrix least-squares on F^2
Observed reflections [$I > 2\sigma(I)$]	4835
Data/restraints /parameters	6032/0/353
Maximum/minimum transmission	0.9374/0.8939
Goodness-of-fit on F^2	1.096
Final R indices [$I > 2\sigma(I)$]	$R_1 = 0.0408$, $wR_2 = 0.0859$
R indices (all data)	$R_1 = 0.0537$, $wR_2 = 0.0920$
Largest different peak and hole	0.687 and −0.425 e Å^{-3}

methods and successive Fourier difference syntheses thermal parameters for all non-hydrogen atoms (SHELXL-97) [13]. Hydrogen atoms were added theoretically and refined with riding model position parameters and fixed isotropic thermal parameters. Further details of structure analysis are given in Table 1. Selected bond lengths and angles are listed in Table 2. Crystallographic data have been deposited with the Cambridge Crystallographic Data Centre as Supplementary Publications Nos. CCDC-630778. Copies of the data can be obtained free of charge on application to CCDC, 12 Union Road, Cambridge CB2, 1EZ, UK (Fax: +44 1223/336 033; E-mail, deposit@ccdc.cam.ac.uk).

Table 2
Selected bond lengths (Å) and angles (°) for NiL[3b]

Ni(1)–N(1)	1.8540(16)	Ni(1)–N(2)	1.8566(17)
Ni(1)–N(4)	1.8548(17)	Ni(1)–N(3)	1.8863(16)
O(1)–C(1)	1.225(2)	N(1)–C(1)	1.365(3)
O(2)–C(2)	1.226(2)	N(1)–C(22)	1.392(3)
O(3)–C(23)	1.204(2)	N(2)–C(2)	1.366(3)
O(4)–C(23)	1.329(2)	N(2)–C(3)	1.390(3)
O(4)–C(24)	1.473(2)	N(3)–C(9)	1.298(3)
O(5)–C(26)	1.204(2)	N(3)–C(10)	1.511(2)
O(6)–C(26)	1.328(2)	N(4)–C(16)	1.292(3)
O(6)–C(27)	1.472(2)	N(4)–C(15)	1.477(2)
C(1)–C(2)	1.534(3)	C(27)–H(27B)	0.9900
H(27B)···O(2)[a]	2.369	C(27)···O(2)[a]	3.349
N(1)–Ni(1)–N(2)	85.54(7)	C(1)–N(1)–C(22)	122.38(17)
N(4)–Ni(1)–N(2)	173.49(7)	C(1)–N(1)–Ni(1)	110.84(13)
N(1)–Ni(1)–N(3)	178.44(7)	C(22)–N(1)–Ni(1)	126.46(13)
N(4)–Ni(1)–N(3)	87.18(7)	C(2)–N(2)–C(3)	122.52(17)
N(2)–Ni(1)–N(3)	95.44(7)	C(2)–N(2)–Ni(1)	110.90(13)
C(27)–H(27B)···O(2)[a]	136.3	C(3)–N(2)–Ni(1)	126.38(14)

[a] Symmetry transformation: −x+1/2, y−1/2, −z+1/2.

2.4. Circular dichronism study

The CD spectra of DNA in the presence or absence of the nickel(II) complexes were collected after 12 h incubation of 0.5 mM CT DNA with 0.2 mM individual nickel(II) complexes in Tris–HCl buffer (pH 7.0) containing 10 mM NaCl at 37 °C. All CD experiments were performed on a Jasco J-715 spectropolarimeter at room temperature from 340 to 230 nm. For each spectrum, three scans were collected with 0.2 nm/data step resolution and as scan speed of 50 nm/min.

2.5. DNA binding studies by competitive fluorescence displacement assay

No-covalent interactions of nickel complexes with double-stranded DNA were studied by titrating the highly fluorescent ethidium–DNA complex with nickel complexes and measuring the decrease in fluorescence. All fluorescence measurements were made using Hitachimodel RF-4500 spectrofluorimeter. DNA and ethidium bromide were combined to give 10 mL of reaction mixtures containing 1.1 μM ethidium bromide (EB), 3.9 μM CT DNA and various concentrations of nickel complexes. The reaction mixtures were excited at 552 nm and the fluorescence intensities at 624 nm were recorded.

2.6. DNA cleavage studies

The reaction mixtures (25 μL total volume) contained 10 ng/μL of supercoiled plasmid (pBR 322 DNA), 10 mM Tris–HCl buffer (pH 7.0), 10 mM NaCl, 0.6 mM individual metal complexes and 15 mM H_2O_2. Reaction mixtures were incubated at 37 °C for 2 h, and then quenched by the addition of 5 μL loading buffer (0.25% bromophenol blue, 0.25% xylene cyanol, 30% glycerol, 10 mM EDTA). 20 μL of samples were loaded onto a 1% agarose gel containing ethidium bromide (1 μg/mL) in TBE buffer (90 mM Tris–borate, pH 8.0, 20 mM EDTA). The gel was run at 120 V for 1 h and photographed under UV light. Quantitation of cleavage products was performed by Glyko BandScan software, Version 4.30. Supercoiled plasmid DNA values were corrected by a factor 1.3, based on average literature estimate of lowered binding of ethidium to this structure [14].

3. Results and discussion

3.1. Description of the structure of the nickel(II) complexes

Six closely related Schiff base macrocyclic oxamido nickel(II) complexes have been synthesized. In general, the molecular structural differences of these mononuclear

complexes lie in the ester moieties and the alkyl moieties connecting the two imino groups. The other moieties of the mononuclear structures are very similar. According to their ester moieties, the six nickel complexes are divided into two groups: group A using methyl ester (NiL^{1a}, NiL^{2a}, NiL^{3a}) and group B using ethyl ester (NiL^{1b}, NiL^{2b}, NiL^{3b}). The difference of the three complexes in each group is the alkyl moieties connecting the two imino groups. The most striking structure feature of NiL^{3a} and NiL^{3b} is of a bulky hydrophobic cyclohexylene moiety.

The crystal structures of NiL^{1a}, NiL^{1b}, and NiL^{2b} have been described previously [15–17]. Here we reported the crystal structure of NiL^{3b}. The molecular structure and atomic numbering of NiL^{3b} are given in Fig. 1. The macrocyclic ligand coordinates to the central Ni(II) ion through its two deprotonated oxamido nitrogen and two imine nitrogen atoms to form a slightly distorted square-planar geometry. The deviations of the four donor atoms (N1 to N4) from their mean plane are −0.0604, 0.0582, −0.0568, 0.0590 Å, respectively. The Ni(II) ion is −0.0382 Å out of the plane. The two phenyl ring moieties of the macrocyclic ligand are not coplanar with the above coordination plane (N1 to N4) and bend to the same side. The dihedral angles between the coordination plane and the two phenyl rings are 19.8° (C3 to C8) and 25.4° (C17 to C22), respectively. The cyclohexylene moiety and the plane (O1, C1, C2, O2) of the two carbonyl groups bend to the other side. The cyclohexylene moiety is nearly perpendicularity to the coordination plane. The plane (O1, C1, C2, O2) bends to the coordination plane with a dihedral angle of 29.1°. The N–C bond lengths (N1–C1 = 1.365(3) Å, N1–C22 = 1.392(3) Å, N2–C2 = 1.366(3) Å, N2–C3 = 1.390(3) Å) involving the oxamido nitrogen atoms are apparently longer than the double bonds (N3–C9 = 1.298(3) Å, N4–C16 = 1.292(3) Å), and obviously shorter than the single bonds (N3–C10 = 1.511(2) Å, N4–C15 = 1.477(2) Å). The oxamido nitrogen atoms and their bonding atoms are of good planarity. The mean deviations from plane (N1, C1, C22, Ni1) and plane (N2, C2, C3, Ni1) are of 0.0185 and 0.0145 Å, respectively. It indicates that the oxamido nitrogen atoms are sp^2-hybridized and the p-electrons on the nitrogen atoms are delocalized to form a conjugated system with the adjacent carbonyls and phenyl rings. As depicted in Fig. 2 and Table 2, the adjacent monomolecules are linked head to tail by the weak C–H···O hydrogen bonds between the ester carbon atom (C27) and

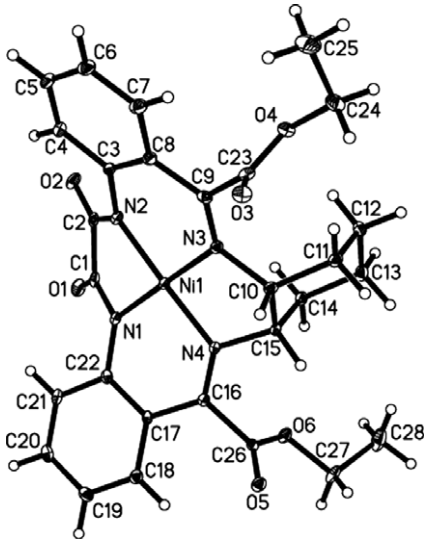

Fig. 1. ORTEP view of the molecular structure and atom-labeling scheme of NiL^{3b}. Thermal ellipsoids are drawn at the 30% probability level.

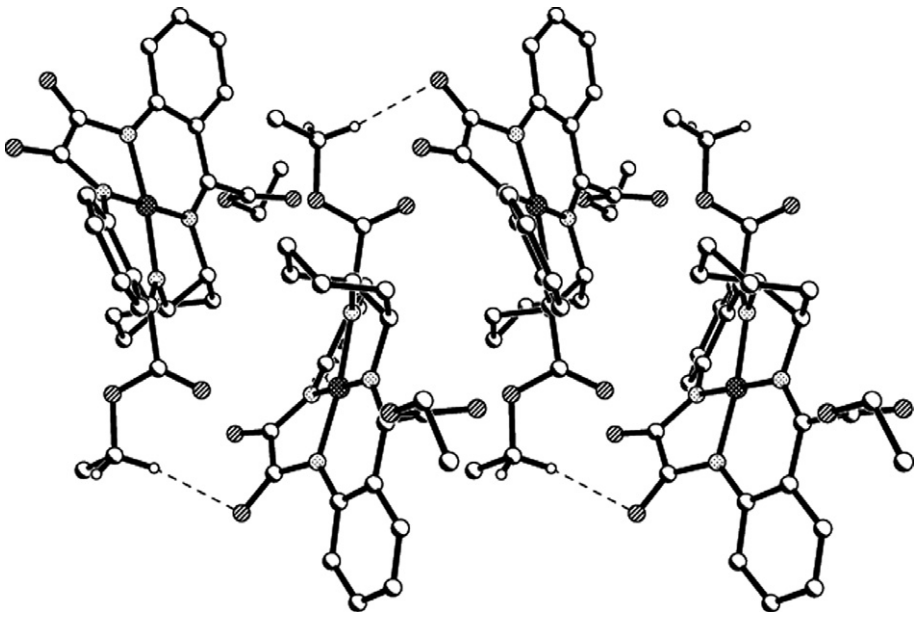

Fig. 2. The supramolecular 1D chain of NiL^{3b} constructed by C-H···O hydrogen bonds. Hydrogen atoms except those involving in hydrogen bonds are omitted for clarity.

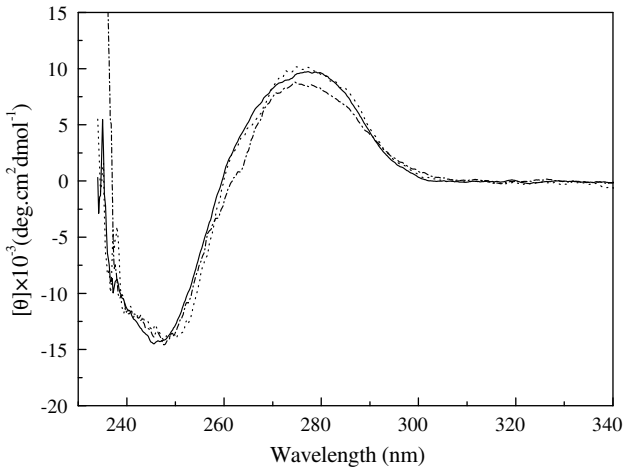

Fig. 3. CD spectra of CT DNA at 0.5 mM (as bp) in the absence (—) and presence of 0.2 mM of NiL^{3a} (····) and NiL^{3b} (—·—·—). (NiL^{1a}, NiL^{1b}, NiL^{2a} and NiL^{2b} have similar influence on the CD spectra of CT DNA to NiL^{3a} and NiL^{3b}, and corresponding CD spectra omitted for clarity).

the oxamido oxygen atom (O2) into a 1D supramolecular chain.

3.2. Nickel(II) complexes–DNA interaction studies

3.2.1. CD spectral studies

The CD spectra of DNA in the absence or presence of nickel(II) complexes were collected after 12 h incubation of CT DNA with individual nickel(II) complexes. Free helix DNA shows the well-known features of a so-called right-handed B form CD spectrum: a positive band at 277 nm due to base stacking and a negative band at 245 nm due to helicity [18]. It has been reported that the changes in CD signals of DNA observed on interaction with small molecules may often be assigned to the corresponding changes in DNA structure. The Intercalation of small molecules to DNA can stabilize the right-handed B conformation of CT DNA, and enhance the intensities of both the bands. Simple groove binding and electrostatic interaction of small molecules with DNA shows little or no perturbations on the two bands [19]. As shown in Fig. 3, similar CD spectra were observed for CT DNA, either with or without the presence of the nickel(II) complexes, which suggests that the interaction of the studied nickel(II) complexes with DNA is a classical non-intercalative mode. This suggestion can also be supported by the crystal structures of the six nickel(II) complexes. In the complexes, the two phenyl ring moieties of the macrocyclic ligand are not coplanar with the Ni(II) coordination plane and bend to the same side [15–17]. It indicates that the complexes cannot be regarded as good intercalative drugs for their poor planarity. However, since all the six complexes contain aromatic rings in their ligand structure, partial intercalation of those molecules cannot be fully ruled out [20].

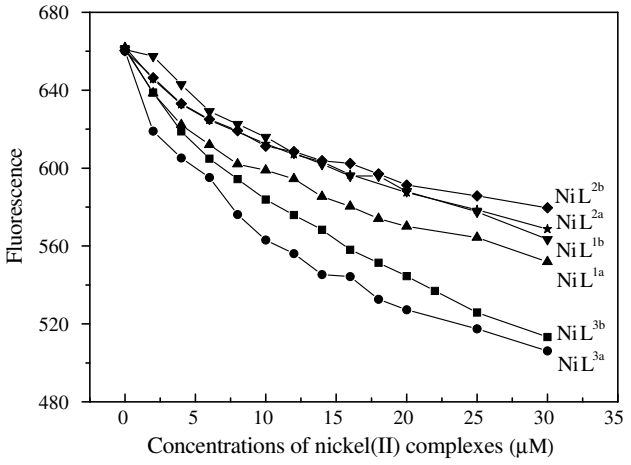

Fig. 4. Fluorescence emission spectra of EB–DNA complex at various concentration of each nickel(II) complex.

3.2.2. Fluorescence spectroscopic studies

No detectable fluorescence emission can be observed for the six nickel complexes we studied, so the binding of these complexes to DNA can not be directly presented in fluorescence emission spectra. It has been previously reported that EB strongly fluoresces when intercalated into DNA, and this enhanced fluorescence can be quenched at least partially by the addition of a second molecule [21]. An experimental strategy for determining binding events for these second molecules based on quenching of EB fluorescence via a competition for binding sites in DNA has became a standard method in nucleic acid chemistry. To determine the binding event of the nickel(II) complexes, we performed fluorescence-quenching experiments with EB-bound DNA. As shown in Fig. 4 the increasing of the concentrations of each nickel(II) complex results in a gradual decrease in fluorescence intensity of the EB-DNA complex, indicating that all of the six complexes we studied can displace EB bound to DNA. This behavior suggests that groove binding interactions would occur between the nickel(II) complexes and DNA [22,23], since the CD spectral analysis excludes the intercalation between them. The six complexes display different abilities of kicking out EB from DNA, which follows the order NiL^{3a} ≈ NiL^{3b} > NiL^{1a} ≈ NiL^{1b} ≈ NiL^{2a} ≈ NiL^{2b}. The higher abilites of NiL^{3a} and NiL^{3b} may be attributed to the DNA groove binding of alicyclic ring (cyclohexylene moiety) as found in Taxol–DNA interaction [24]. Group A has a little higher ability of displacing EB from DNA than group B, such as NiL^{1a} vs. NiL^{1b}, NiL^{2a} vs. NiL^{2b}, NiL^{3a} vs. NiL^{3b}. This behavior may be attributed to the steric encumbrance of bulky ethyl ester substituent in group B.

3.3. Oxidative cleavage of DNA

3.3.1. DNA Cleavage activity comparison of the six nickel(II) complexes

In order to assess the competence of the six nickel(II) complexes for DNA strand scission, pBR 322 DNA was

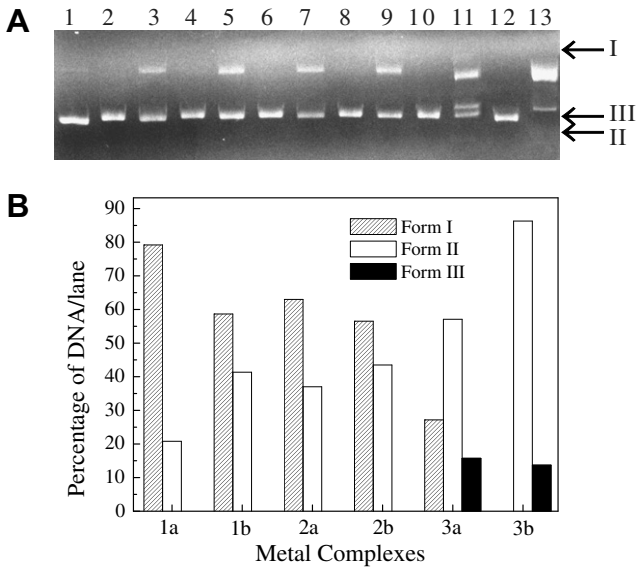

Fig. 5. Oxidative cleavage of pBR 322 DNA by different nickel(II) complexes. (A) Gel electrophoresis results. Lanes are 1, DNA control; 2 and 3, NiL^{1a}; 4 and 5, NiL^{1b}; 6 and 7, NiL^{2a}; 8 and 9, NiL^{2b}; 10 and 11, NiL^{3a}; 12 and 13, NiL^{3b}. Each pair of lanes shows the cleavage experiment in absence and in presence of H_2O_2, respectively. (B) Densitometric quantitative results of the gel electrophoresis.

incubated with individual nickel(II) complexes under identical reaction conditions. The cleavage reaction can be monitored by gel electrophoresis. When circular pBR 322 DNA is subjected to electrophoresis, relatively fast migration will be observed for the intact supercoiled form (Form I). If scission occurs on one strand (nicking), the supercoiled form will relax to generate a slower-moving nicked form (Form II). If both strands are cleaved, a linear form (Form III) that migrates between Form I and Form II will be generated.

As shown in Fig. 5, all of the examined complexes are capable of promoting oxidative damage of DNA in the presence of H_2O_2 under physiological conditions (pH 7.0, 37 °C), but display different cleavage activities. NiL^{3b} exhibits the highest DNA cleavage activity. Under the conditions we used, it can completely convert supercoiled form to nicked and linear form of DNA. NiL^{3a} also can convert supercoiled DNA to nicked and linear DNA, but the supercoiled form is still seen. The difference in cleavage behavior of the two complexes appears to be due to the ester moieties, since the molecules are matched in all other respects. NiL^{1a}, NiL^{1b}, NiL^{2a}, NiL^{2b} are less effective than NiL^{3a} and NiL^{3b}. These four complexes can only convert supercoiled form to nicked form. The difference in cleavage characteristics of these four complexes versus NiL^{3a} and NiL^{3b} appears to be due to the cyclohexylene moiety of NiL^{3a} and NiL^{3b}. From Fig. 5B we can find that the cleavage ability of NiL^{1b} is a little higher than that of NiL^{1a}, and NiL^{2b} a little higher than NiL^{2a}. This difference can also be attributed to the presence of ethyl ester substitutes in NiL^{1b} and NiL^{2b}. The control experiments were carried out in the presence of individual complexes together with DNA and in the absence of H_2O_2 showed no background cleavage.

3.3.2. Effects of ionic strength on plasmid DNA cleavage

Fig. 6 shows the results of an ionic strength study in which pBR 322 DNA is treated with NiL^{3b} under conditions of increasing ionic strength through added NaCl. From this figure we can see that the process of DNA cleavage is sensitive to the change of ionic strength. Both nicked and linear DNA decrease with the increasing of ionic strength, and the process of linearization seems to be more sensitive to increasing ionic strength than that of nicking. Virtually no linear DNA can be observed above 10 mM added NaCl, while substantial amounts of nicked DNA continue to occur even at 200 mM added NaCl. These results imply that the electrostatic interaction can influence the DNA cleavage reaction in some degree.

3.3.3. Effects of pH on plasmid DNA cleavage

In order to further investigate the electrostatic contribution to DNA cleavage, the effect of pH on DNA cleavage was explored. From Fig. 7 we can find that the process of DNA cleavage is only slightly influenced by changing the value of pH. It seems that the extents of DNA cleavage under basic conditions are a little higher than those under acidic and neutral conditions. This result may indicate the involvement of reactive oxygen species in the mechanism for DNA cleavage by the examined complexes. It has been proven that some reactive oxygen species, such as hydroxyl radicals, may be produced during the reactions of metal complexes with DNA, and these reactive oxygen species may be responsible for the oxidative DNA cleavage. It is well known that high pH conditions may be favorable for the formation of such reactive oxygen species [25,26].

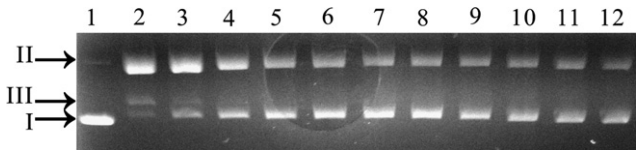

Fig. 6. Ionic strength dependence of NiL^{3b}-mediated DNA cleavage. Lane 1, DNA control; lane 2–12, 0, 5, 10, 20, 40, 60, 80, 100, 120, 160, 200 mM NaCl added to reaction mixture. In this experiment, the reaction time is 60 min.

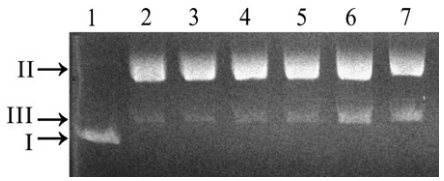

Fig. 7. pH dependence of NiL^{3b}-mediated DNA cleavage. Lanes are l, DNA control; 2, pH 4.0; 3, pH 5.0; 4, pH 6.0; 5, pH 7.0; 6, pH 8.0; 7, pH 9.0.

3.3.4. Effects of reaction time on plasmid DNA cleavage

The experiment to explore time dependence of NiL^{3b}-mediated DNA cleavage was also carried out at physiological pH and temperature. The fragments produced in the presence of NiL^{3b} were analyzed by electrophoresis (Fig. 8A) and a plot of the percentage of either DNA form versus reaction time was obtained by using the electrophoresis data (Fig. 8B). From these figures, we can find that treatment of plasmid DNA with NiL^{3b} results in exponential conversion of supercoiled DNA to nicked DNA. After treatment with NiL^{3b} for 30 min, linear DNA is also observed. Supercoiled DNA completely disappears after 80 min. That is to say, NiL^{3b} can convert supercoiled DNA to nicked DNA then linear DNA in a sequential manner. From Fig. 8B we can find this is a typical pseudo-first-order consecutive reaction, which is consistent with the general model for enzyme catalyzed reactions [27]. Fitting the experimental data with first-order consecutive kinetic equations, the rate constants of $3.27 \pm 0.14\ h^{-1}$ (k_1) and $0.0966 \pm 0.0042\ h^{-1}$ (k_2) for the conversion of supercoiled to nicked DNA and nicked to linear DNA are obtained, respectively. Since the rate constant k_1 is much larger than k_2, NiL^{3b} may be said to be a single strand cleavage agent, and the cleavage is nonspecific [28].

3.3.5. Effects of complex concentration on plasmid DNA cleavage

In order to investigate the influence of the concentration of the NiL^{3b} or H_2O_2 on DNA cleavage reactions, three independent experiments were explored. In the first experiment, the concentration of H_2O_2 was kept constant and the concentration of the complexes was varied (Fig. 9A); in the second experiment, the concentration of the complexes was kept constant and the concentration of H_2O_2 was varied (Fig. 9B); in the third experiment, the concentration of the complexes and H_2O_2 was changed synchronously, and their concentration ratio was kept constant (Fig. 9C). All of the results indicate that the DNA cleavage activities of the complexes are obviously both complex and H_2O_2 concentration-dependent. With the increase in complex or H_2O_2 concentration, the supercoiled DNA decreases and is finally completely converted to nicked and linear forms.

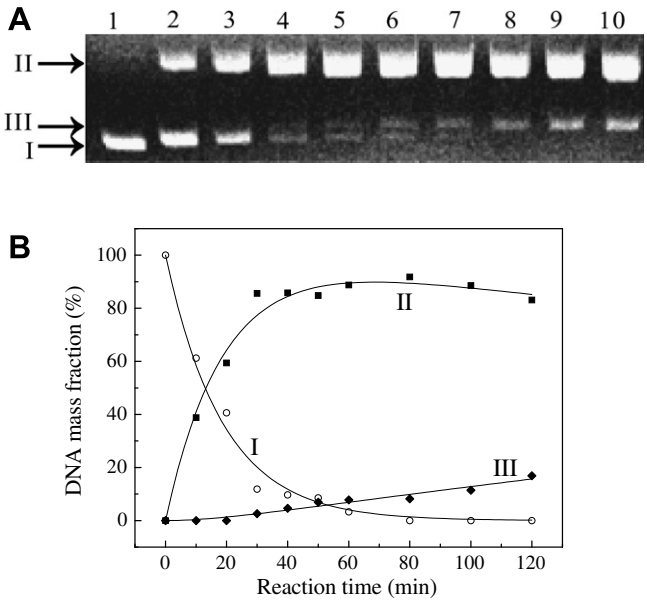

Fig. 8. Reaction time dependence of NiL^{3b}-mediated DNA cleavage. (A) Gel electrophoresis results. The reaction time for lane 1–10 was 0, 10, 20, 30, 40, 50, 60, 80, 100, 120 min, respectively. (B) Densitometric quantitative results of the gel electrophoresis. Scatter: experimental data, line: fitting curves.

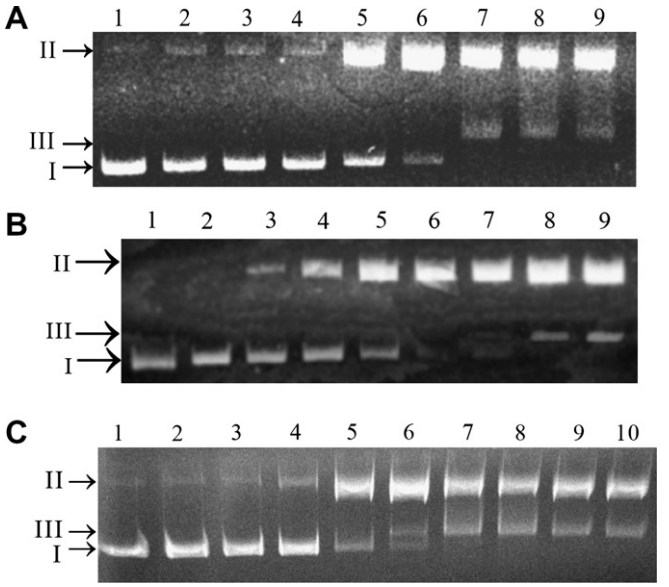

Fig. 9. DNA cleavage by various concentration of NiL^{3b}. (A) The concentration of H_2O_2 is kept constant at 15 mM and the concentration of NiL^{3b} is varied. Lane 1, DNA control; lane 2–9, 0, 0.04, 0.08, 0.16, 0.24, 0.32, 0.40, 0.48 mM NiL^{3b} added to reaction mixtures. (B) The concentration of NiL^{3b} is kept constant at 0.60 mM and the concentration of H_2O_2 is varied. Lane 1, DNA control; lane 2–9, 0, 1.0, 2.0, 4.0, 6.0, 8.0, 12.0, 15.0 mM H_2O_2 added to reaction mixtures. (C) The concentration ratio of H_2O_2 to NiL^{3b} is kept constant at 25 and the NiL^{3b} concentration is varied. lane1, DNA control l; lane 2–10, 0, 0.08, 0.16, 0.24, 0.32, 0.40, 0.48, 0.56, 0.64 mM NiL^{3b} added to reaction mixtures.

3.3.6. Effects of radical scavengers on plasmid DNA cleavage

To investigate whether reactive oxygen species, such as singlet oxygen and hydroxyl radicals, were involved in

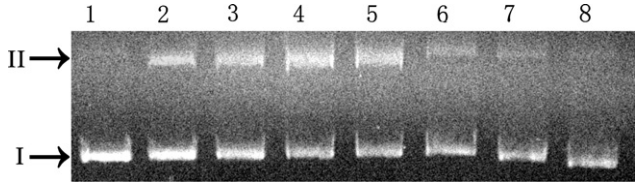

Fig. 10. DNA cleavage by NiL^{3b} in presence of different radical scavengers. $[NiL^{3b}] = 0.40$ mM, $[H_2O_2] = 10$ mM. Lanes are 1, DNA control; 2, no scavenger; 3, 150 μM sodium azide; 4, 1.2 mM histidine; 5, 0.7 M ethanol; 6, 0.55 M glycerol; 7, 1.13 M DMSO; 8, 150 μM KI. In this experiment, the reaction time is 30 min.

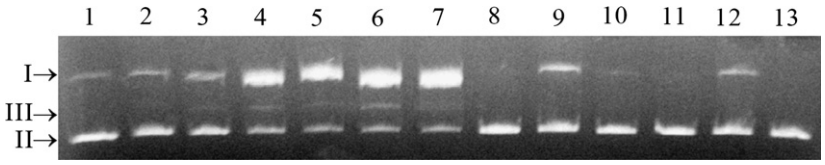

Fig. 11. DNA cleavage by different nickel(II) in presence of different DNA groove binding drugs. Lanes are 1, DNA control; 2, 1000 U SYBR Green; 3, 0.4 mM methyl green; 4, 0.40 mM NiL^{3b} + 1000 U SYBR Green; 5, 0.40 mM NiL^{3b}; 6, 0.40 mM NiL^{3b} + 0.4 mM methyl green; 7. 0.40 mM NiL^{3b} + 1000 U SYBR Green + 0.4 mM methyl green; 8, 0.40 mM NiL^{2b} + 1000 U SYBR Green; 9. 0.40 mM NiL^{2b}; 10. 0.40 mM NiL^{2b} + 0.4 mM methyl green; 11. 0.40 mM NiL^{1b} + 1000 U SYBR Green; 12. 0.40 mM NiL^{1b}; 13. 0.40 mM NiL^{1b} + 0.4 mM methyl green.

DNA cleavage, the effects of several radical scavengers were examined. As shown in Fig. 10, no obvious inhibitions are observed in the presence of singlet oxygen scavengers, such as sodium azide and histidine, indicating that singlet oxygen is not likely to be the reactive species. Among the hydroxyl radical scavengers we studied, dimethyl sulfoxide (DMSO), glycerol, and potassium iodide inhibit DNA cleavage, whereas ethanol does not. A similar result has been previously reported [29]. These results confirm the involvement of $OH^{\cdot}$ in the reaction, which is consistent with the result of the pH study. The difference in the prohibitive abilities of different hydroxyl radical scavengers may suggest that hydroxyl radicals are generated in close association with DNA such that ethanol cannot remove them. According to the results mentioned above, we hypothesis that the examined nickel(II) complex may be capable of promoting DNA cleavage through a direct oxidative DNA damage pathway that has been reported, in which the reactive species may be a Ni(III)-peroxide complex, which can release hydroxyl radicals [29].

3.3.7. Effects of groove binding drugs on plasmid DNA cleavage

It has been proposed that the DNA binding ability of some metal complexes was essential to mediate DNA cleavage when reactive oxygen species acted as the oxidative intermediates [11]. The results of fluorescence spectroscopic studies (Fig. 4) showed that NiL^{3a} and NiL^{3b} had higher DNA binding abilities than other four complexes. In order to investigate whether the higher DNA binding abilities of NiL^{3a} and NiL^{3b} are relevant to their higher DNA cleavage abilities, the effect of groove binding drugs on the strand scission was also determined. As shown in Fig. 11, the addition of SYBR Green and methyl green, which are known to interact to DNA at minor and major groove, respectively [10,30], hardly inhibited DNA cleavage by NiL^{3b} but completely inhibited DNA cleavage by NiL^{1b} or NiL^{2b}. Similar results were obtained for the three complexes in group A. These results can partly reflect the binding interaction between the nickel(II) complexes and DNA. Because of the presence of planar aromatic rings, these nickel(II) complexes may partially intercalate into base pairs of DNA, and this partial intercalation may be the dominant binding mode between DNA and NiL^{1b} or NiL^{2b}. This binding mode will be favorable to the accessibility of nickel ion to cleavage sites. The addition of either minor or major groove drug can hinder the partial intercalation of aromatic rings into DNA, hinder the accessibility of nickel ion to cleavage sites, and then completely inhibit the DNA cleavage. Besides partial interaction, groove binding is also an important binding mode between NiL^{3b} and DNA. As NiL^{1b} and NiL^{2b}, the binding interaction between NiL^{3b} and DNA certainly effects the DNA cleavage reactions by NiL^{3b} in some degree. But this effect is overwhelmed by some other factors such as redox ability and conformational flexibility of the complex. Thus, the addition of SYBR Green and methyl green seems to have no effect on DNA cleavage ability of NiL^{3b}. From these results we can suggest that the binding interaction between the nickel(II) complexes and DNA may affect the DNA cleavage abilities of the complexes in some degree, but it is not the dominant factor in determining reactivity.

4. Conclusions

Six closely related Schiff base macrocyclic oxamido nickel(II) complexes have been synthesized and their abilities to induce oxidatively generated DNA damage were compared. The agarose gel electrophoresis studies show that all of these complexes can promote the oxidative cleavage of plasmid DNA at physiological pH and temperature in the presence of H_2O_2, and but the reactivity is highly dependent upon the macrocyclic ligand employed. CD, fluorescence spectroscopy and gel electrophoresis indicate that the complexes bind to DNA by partial intercalative and groove binding modes, but these binding interactions are not the dominant factor in determining the DNA cleavage abilities of the complexes. The study of these closely related nickel(II) complexes may provide some important information not only for elucidating the relationship between the structures of nickel(II) complexes and their DNA reactive activities, but also for the chemistry of nickel-based nucleolytic agents.

5. Abbreviations

CD	circular dichronism
CT DNA	calf thymus DNA
EDTA	ethylenediaminetetraacetic acid
TBE	tris–borate–EDTA
EB	ethidium bromide

DMSO dimethyl sulfoxide
UV ultraviolet

Acknowledgments

This work was supported by the National Natural Science Foundation of China (Nos. 20405007 and 20675041), the National Basic Research Program of China (No. 2006CB705700).

Appendix A. Supplementary data

Supplementary data associated with this article can be found, in the online version, at doi:10.1016/j.jinorgbio.2007.12.002.

References

[1] K. Dhara, J. Ratha, M. Manassero, X.-Y. Wang, S. Gao, P. Banerjee, J. Inorg. Biochem. 101 (2006) 95–103.
[2] S. Arounaguiri, D. Easwaramoorthy, A. Ashokkumar, A. Dattagupta, B.G. Maiya, Proc. Indian. Acad. Sci. (Chem. Sci.) 112 (2000) 1–17.
[3] Chem. Rev. 98 (1998) 937–1262: thematic issue (no. 3) on RNA/DNA cleavage.
[4] J.G. Muller, X. Chen, A.C. Dadiz, S.E. Rokita, C.J. Burrows, J. Am. Chem. Soc. 114 (1992) 6407–6411.
[5] S.S. Matkar, L.A. Wrischnik, P.R. Jones, U. Hellmann-Blumberg, Biochem. Biophys. Res. Commun. 343 (2006) 754–761.
[6] H. Lu, X. Shi, M. Costa, C. Huang, Mol. Cell. Biochem. 279 (2005) 45–67.
[7] M.C. Rodrìguez-Argüelles, M.B. Ferrari, F. Biscegli, C. Pellizi, G. Pelosi, S. Pinelli, M. Sassi, J. Inorg. Biochem. 98 (2004) 313–321.
[8] Z. Afrasiabi, E. Sinn, W. Lin, Y. Ma, C. Campana, S. Padhye, J. Inorg. Biochem. 98 (2005) 1526–1531.
[9] L.-Z. Li, C. Zhao, T. Xu, H.-W. Ji, Y.-H. Yu, G.-Q. Guo, H. Chao, J. Inorg. Biochem. 99 (2005) 1076–1082.
[10] F.B. El Amrani, L. Perelló, J.A. Real, M. González-Alvarez, G. Alzuet, J. Borrás, S. García-Granda, J. Montejo-Bernardo, J. Inorg. Biochem. 100 (2006) 1208–1218.
[11] Y. Zhao, J. Zhu, W. He, Z. Yang, Y. Zhu, Y. Li, J. Zhang, Z. Guo, Chem. Eur. J. 12 (2006) 6621–6629.
[12] D.S.C. Black, G.I. Moss, Aust. J. Chem. 40 (1987) 129–142.
[13] G.M. Sheldrick, SHELXS-97 and SHELXL-97, Software for Crystal Structure Analysis, Siemens Analytical X-ray Instruments Inc., Madison, WI, 1997.
[14] F.V. Pamatong, C.A. Detmer, J.R. Bocarsly, J. Am. Chem. Soc. 118 (1996) 5339–5345.
[15] X.-Z. Li, D.-Z. Liao, Z.-H. Jiang, S.-P. Yan, Chin. J. Struc. Chem. 22 (2003) 293–296.
[16] X.-Z. Li, G.-M. Yang, D.-Z. Liao, Z.-H. Jiang, S.-P. Yan, J. Crystallogr. Chem. 33 (2003) 5–9.
[17] X.-Z. Li, J.-H. He, B.-L. Liu, D.-Z. Liao, Inorg. Chem. Commun. 7 (2004) 420–422.
[18] A. Rajendran, B.U. Nair, Biochim. Biophys. Acta 1760 (2006) 1794–1801.
[19] P. Uma Maheswari, M. Palaniandavar, J. Inorg. Biochem. 98 (2004) 219–230.
[20] V. Uma, A. Castineiras, B.U. Nair, Polyhedron 26 (2007) 3008–3016.
[21] C. Liu, J. Zhou, H. Xu, J. Inorg. Biochem. 71 (1998) 1–6.
[22] B.C. Baguley, E.M. Falkenhaug, Nucleic Acids Res. 5 (1978) 161–171.
[23] B.F. Cain, B.C. Baguley, W.A. Denny, J. Med. Chem. 21 (1978) 658–668.
[24] A.G. Krishna, D.V. Kumar, B.M. Khan, S.K. Rawal, K.N. Ganesh, Biochim. Biophys. Acta 1381 (1998) 104–112.
[25] N. Saglam, A. Colak, K. Serbest, S. Dülger, S. Güner, S. Karaböcek, A.O. Beldüz, Biometals 15 (2002) 357–365.
[26] X. Shi, N.S. Dalal, K.S. Kasprzak, Arch. Biochem. Biophys. 302 (1993) 294–299.
[27] J.J. Li, R. Geyer, W. Tan, Nucleic Acid Res. 28 (2000) e52.
[28] J. Googisman, C. Krik, J.C. Dabrowiak, Biophys. Chem. 69 (1997) 249–268.
[29] S. Kawanishi, S. Olikawa, S. Ioue, K. Nishino, Environ. Health Perspect. 110 (2002) 789–791.
[30] D. Gibellini, F. Vitone, P. Schiavone, C. Ponti, M.L. Placa, M.C. Re, J. Clin. Virol. 29 (2004) 282–289.